NJC

PAPER

View Article Online
View Journal | View Issue

Check for updates

Cite this: *New J. Chem.*, 2019, **43**, 16945

Tracking mitochondrial viscosity in living systems based on a two-photon and near red probe†

Min Peng, Junling Yin and Weiying Lin *

Received 18th July 2019,
Accepted 16th September 2019

DOI: 10.1039/c9nj03744f

rsc.li/njc

A two-photon fluorescent probe, **Mito-V,** was designed and prepared for sensing the viscosity changes of mitochondria. The systematic investigations demonstrated that the fluorescence emission at 634 nm increased about 22-fold from methanol to 99% glycerol, indicating high viscosity dependence. Notably, using the probe, the mitochondrial viscosity fluctuations have been successfully monitored not only in living cells but also in zebrafish and living mice.

Published on 04 October 2019. Downloaded by University of Georgia on 1/3/2020 6:36:17 AM.

Viscosity, as one of the crucial parameters of cells, directly affects the interaction between the transmission of chemical signals and intracellular biomolecules as well as facilitating the diffusion of metabolites.[1,2] Mitochondria, as a vital intracellular organelle, are present in the cytoplasm of almost all eukaryotic cells, and they play an important role in maintaining the balance of numerous physiological functions in human physiology.[3–5] Additionally, mitochondria are known as the cellular energy factory due to the fact that their principal function is energy production. Deviation from normal mitochondrial viscosity levels will result in inactivation of mitochondria, which will trigger various diseases including diabetes, atherosclerosis, Parkinson's disease (PD) and Alzheimer's disease (AD).[6–13] To this end, developing a targeted molecule capable of real-time monitoring the mitochondrial viscosity is crucial to better understand the mechanism of mitochondria during pathological and biological processes.

Recently, various viscometers have been developed to detect viscosity. Unfortunately, these traditional methods fail to measure the viscosity at the cellular level.[14–16] Compared with traditional techniques, fluorescence technology has become a powerful tool for detecting viscosity in living systems owing to its excellent properties including high sensitivity, non-invasive detection, high selectivity as well as real-time monitoring and temporal resolution.[16–18] In particular, two-photon (TP) fluorescent probes have been developed as robust tools for sensing viscosity variations in biological systems. Compared with one-photon (OP) fluorescent probes, TP fluorescent probes have received more favor with the merits of deeper penetration, higher spatial resolution as well as longer excitation wavelength and lower phototoxicity.[19–22] Thus, it is of great urgency to design a TP fluorescent probe for detecting viscosity variations in the mitochondrial region.

Fluorescent probes typically contain a molecular rotor and a fluorophore. For such a fluorescent probe, molecular rotors can be rotated relative to the fluorophore in non-viscous media providing relaxation of an electronically excited dye by a non-radiative process.[22–27] However, the fluorescence was enhanced in high viscous-media, which was ascribed to the fact that the rotation of the molecular rotor was inhibited and the likelihood of non-radiative pathways was reduced.[28,29] Furthermore, detection of changes in viscosity of a particular organelle can also be achieved by introducing a targeting group.[30,31] Inspired by this, we aimed to design a mitochondrial targeting fluorescent probe that possesses the fluorophore and the rotor with the aim of tracking and sensing mitochondrial viscosity changes in living systems.

Herein, we have rationally designed and synthesized a near red probe, **Mito-V** (Scheme 1), for tracking mitochondrial viscosity

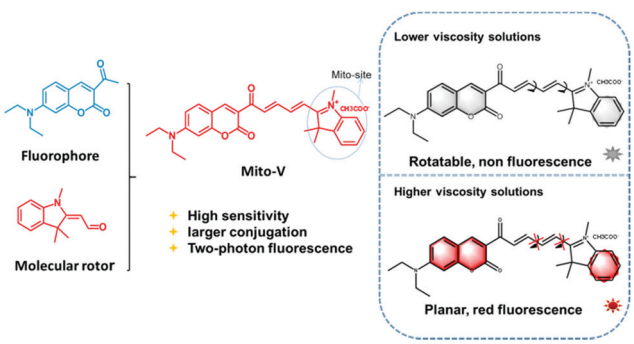

Scheme 1 The design concept of **Mito-V** for monitoring viscosity.

Institute of Fluorescent Probes for Biological Imaging, School of Chemistry and Chemical Engineering, School of Materials Science and Engineering, University of Jinan, Jinan, Shandong 250022, P. R. China. E-mail: weiyinglin2013@163.com

† Electronic supplementary information (ESI) available: Characterization data, and additional spectra. See DOI: 10.1039/c9nj03744f

Published on 04 October 2019. Downloaded by University of Georgia on 1/3/2020 6:36:17 AM.

with two-photon excitation using hemicyanine and coumarin as an acceptor and a donor, respectively. Coumarin, as an excellent donor, is widely used in the synthesis of dyes and two-photon fluorescent probes. Furthermore, hemicyanine, as a mitochondrial targeting group, possesses a positive charge that facilitates penetration into the mitochondria of cells through the plasma membrane. We envision that **Mito-V** would emit no fluorescence in non-viscous media owing to free rotation of the coumarin moiety and hemicyanine moiety. However, the rotation would be restricted and the fluorescence intensity would become dramatically enhanced in highly viscous media. Therefore, **Mito-V** may be suitable for monitoring mitochondrial viscosity.

With the successful preparation of the probe, the optical properties of **Mito-V** in a mixture of glycerol–methanol were investigated. Firstly, we measured the UV-vis absorption spectrum of **Mito-V** in glycerol and methanol solutions, respectively (Fig. S1, ESI†); **Mito-V** exhibited slightly heightened fluorescence from methanol to glycerol solution. As expected, **Mito-V** exhibited negligible fluorescence in methanol (Fig. 1a). However, the fluorescence emission intensity at λ_{ex} = 634 nm of **Mito-V** exhibited a remarkable increase by *ca.* 22-fold upon viscosity changing from 1.7 cP to 953.0 cP. In addition, a good linear relationship exists between $\log I_{634}$ and $\log \eta$ with a correlation coefficient of 0.99 according to the Förster–Hoffmann equation (Fig. 1b), indicating that **Mito-V** is able to detect viscosity. Moreover, the fluorescence quantum yield of **Mito-V** was calculated in different methanol/glycerol fractions and the result is depicted in Fig. 1c and Table S1 (ESI†). A quantum yield of **Mito-V** of 0.0372 was obtained in methanol, an approximately 12-fold enhancement of intensity on going from methanol to glycerol. Moreover, the two-photon action spectra of **Mito-V** were recorded. The maximum TP absorption cross sections of **Mito-V** were obtained at 730 nm with 63 GM (Fig. S2, ESI†) indicating the two-photon nature of the probe **Mito-V**. As anticipated, the probe **Mito-V** also exhibits an obvious viscosity dependence in TP mode (Fig. S3, ESI†). Additionally, considering that the cytoplasm is a complex heterogeneous fluid, polarity would be a potential factor affecting probe behaviour. To confirm whether **Mito-V** is affected by the polarity of the solvent, the fluorescence spectra of **Mito-V** in different polarity solvents were measured. As shown in Fig. 1d, **Mito-V** exhibited almost no fluorescence in different polar solvents compared to strong fluorescence in glycerol, indicating that the probe **Mito-V** was almost completely unaffected by polarity. These results demonstrate that **Mito-V** may be applied for monitoring viscosity changes in complex biological environments.

It is important to evaluate probe selectivity because the cell is a complex multicomponent system, which might generate significant effects on cellular viscosity. Based on this, the fluorescence spectra of **Mito-V** were recorded in the presence of various possible competitive biomolecules. As displayed in Fig. 2a, active nitrogen, anions, cations, active oxygen and amino acids triggered almost no fluorescence fluctuation, indicating the high selectivity of **Mito-V**. Moreover, other spectral experiments have indicated that **Mito-V** exhibits excellent photostability (Fig. S4, ESI†) and negligible fluorescence responses to pH changes (Fig. S5, ESI†). Prior to this, the cytotoxicity of **Mito-V** toward HeLa cells was evaluated by the MTT standard assay. As shown in Fig. 2b, the survival rate of HeLa cells was more than 85%, indicating that **Mito-V** has low toxicity to HeLa cells. These results suggest that **Mito-V** would be suitable for imaging living cells.

Considering the overall positive charge of **Mito-V**, the co-localization experiments of **Mito-V** were performed with Mito-Tracker Green (MTG) by confocal laser microscopy. As shown in Fig. 3, the imaging results indicate that **Mito-V** could easily enter HeLa cells and a clear fluorescence image was obtained in the TRITC channel (570–620 nm) (Fig. 3a). Simultaneously, MTG imaging was collected in the FITC channel (500–550 nm) (Fig. 3b). The merged image indicated that the red TRITC channel of **Mito-V** and the green FITC channel of MTG overlapped pretty well (Fig. 3c). Moreover, the Pearson correlation coefficients were calculated to be as high as 0.92 (Fig. 3d) and the intensity profile variations in the

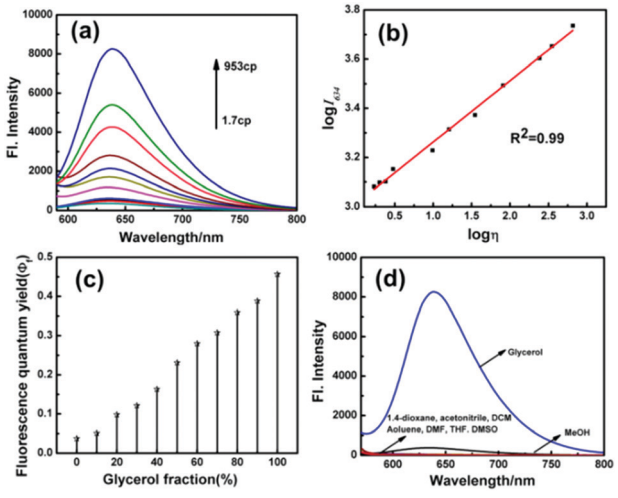

Fig. 1 (a) The fluorescence emission spectra of 10 μM **Mito-V** in the varied viscosity media of methanol/glycerol (v/v) mixtures. (b) Linear relationship of $\log I_{634}$ and $\log \eta$, R^2 = 0.99. (c) Fluorescence quantum yield (Φ_f) of **Mito-V** in the methanol/glycerol (v/v) mixture. (d) Fluorescence emission of **Mito-V** in various solvents with different polarity. The spectra were recorded at 25 °C, the fluorescence intensity was measured at λ_{ex} = 561 nm with both excitation and emission slit widths of 5 nm, and 700 V PMT voltage.

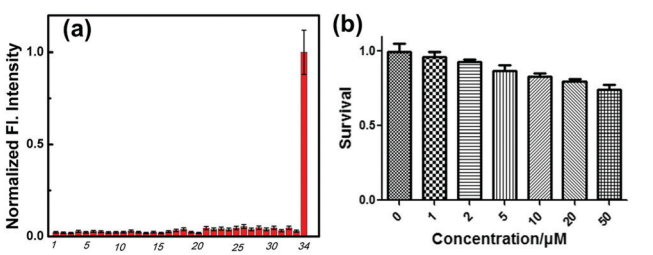

Fig. 2 (a). Fluorescence intensity of **Mito-V** (10 μM) at λ_{em} = 634 nm in PBS buffer (pH = 7.4, 0.01 mM) 1: Ac^-; 2: Br^-; 3: Cl^-; 4: CO_3^{2-}; 5: F^-; 6: HCO^{3-}; 7: HPO_4^-; 8: SO_3^{2-}; 9:SO_4^{2-}; 10: NO^{2-}; 11: Al^{3+}; 12: Ba^{2+}; 13: Ca^{2+}; 14: Co^{2+}; 15: Cu^{2+}; 16: Sn^{2+}; 17: Fe^{2+}; 18: Fe^{3+}; 19: Ni^{2+}; 20: Mg^{2+}; 21: Ala; 22: Arg; 23: Ser; 24: D-alanine; 25: GSH; 26: L-glutamic; 27: Gln; 28: Asp; 29: Val; 30: Thr; 31: Gly; 32: Ile; 33: Leu; 33: Hcy; 34: Glycerol; (b). The cytotoxicity of **Mito-V** in HeLa cells.

 This journal is © The Royal Society of Chemistry and the Centre National de la Recherche Scientifique 2019

Published on 04 October 2019. Downloaded by University of Georgia on 1/3/2020 6:36:17 AM.

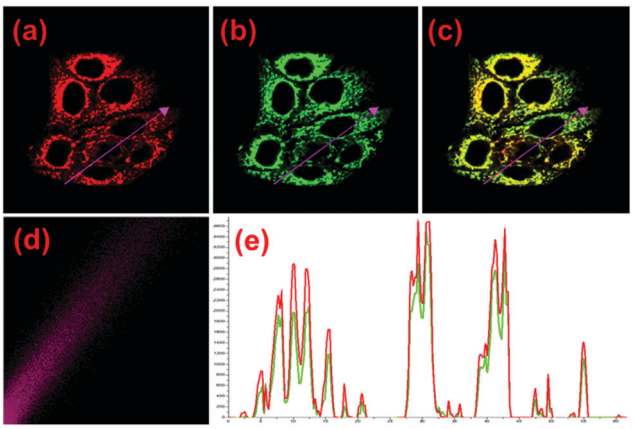

Fig. 3 Co-localization fluorescence images of the probe **Mito-V** in HeLa cells. (a) **Mito-V** (10 μM) stain, λ_{ex} = 561 nm, collected at 570–620 nm. (b) Mitochondrial green stain, λ_{ex} = 488 nm, collected at 500–550 nm. (c) The merged image of (a) and (b). (d) Intensity scatter plots of the probe **Mito-V** across the cells in the red and green channels. (e) Intensity profile of the two channels. Scale bar: 25 μm.

two channels show a synchronous trend (Fig. 3e). As expected, the experimental results indicate that **Mito-V** possesses favourable membrane permeability and specifically accumulates in mitochondria.

Subsequently, the capacity of the probe **Mito-V** for the real-time monitoring of the dynamic changes in mitochondrial viscosity under an external stimulus was validated. External stimuli (monensin and nystatin) were utilized to stimulate a viscosity increase by inducing mitochondrial disorders.[32,33] The cells stained without **Mito-V** exhibited no fluorescence (Fig. 4A(a1–a3)). When the HeLa cells were stained only with **Mito-V**, the probe emitted weak red fluorescence (Fig. 4A(b1–b3)). Excitingly, when the cells were pre-incubated with nystatin or monensin for 30 min and then stained with **Mito-V** for another 30 min, an obvious strong red fluorescence was observed in the TRITC channel (Fig. 4A(c1–c3) and (d1–d3)). Besides, cuvette experiments were carried out with the addition of nystatin or monensin in glycerol or methanol, and the fluorescence exhibited negligible perturbation (Fig. S6, ESI†), indicating that the cellular fluorescence intensity increase can be attributed to viscosity variations in mitochondria rather than the external stimulus. In addition, the analysis results of the cells stimulated by exogenous sources displayed that the average fluorescence intensity was 4.3-fold higher than the normal values in the OP (Fig. 4B) or TP mode (Fig. 4C). More importantly, the quality of the fluorescence image in TP mode is obviously superior to that in OP mode (Fig. S7, ESI†). More importantly, we have performed the real-time fluorescence imaging of dynamic changes in mitochondrial viscosity at different time intervals, indicating that the fluorescence intensity gradually increases with time and remains stable (Fig. S9, ESI†). These phenomena suggest that **Mito-V** can sensitively monitor viscosity of mitochondria in living cells.

Furthermore, based on the above research, we evaluated the feasibility of **Mito-V** for sensing the viscosity changes in zebrafish. The zebrafish were initially non-fluorescent (Fig. 5A(a1–a4)) and weak red fluorescence was observed after treating with **Mito-V** (Fig. 5A(b1–b4)). However, in the presence of the external stimulus (monensin and nystatin), zebrafish emitted stronger red fluorescence (Fig. 5A(c1–c4) and (d1–d4)). Moreover, the analysis results of the zebrafish demonstrated that the mean fluorescence intensity triggered by the external stimulus was 3.1-fold higher than the normal ones in the OP (Fig. 5B) or TP channel (Fig. 5C). Similarly, the quality of the fluorescence image in TP mode is obviously superior to that in OP mode (Fig. S8, ESI†). The above phenomena corresponded well with the results observed in living cell imaging experiments, which further demonstrated that the probe **Mito-V** could be applied for making a distinction between viscous zebrafish and normal zebra-fish by fluorescence imaging of mitochondrial viscosity.

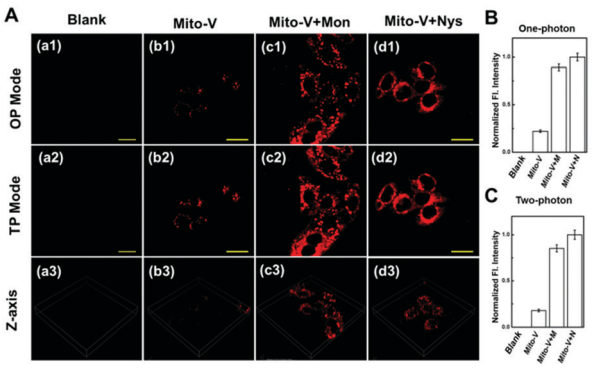

Fig. 4 (A) (a1)–(a3) Confocal fluorescence images of the cells incubated without **Mito-V**. (b1)–(b3) Confocal fluorescence images of the cells incubated with 10 μM **Mito-V**. (c1)–(c3) Confocal fluorescence images of the cells incubated with 10 μM Monensin for 30 min + 10 μM **Mito-V** for another 30 min. (d1)–(d3) Confocal fluorescence images of the cells incubated with 10 μM Nnystatin for 30 min + 10 μM **Mito-V** for another 30 min. (B) Normalized fluorescence intensity of HeLa cells in OP mode. (C) Normalized fluorescence intensity of HeLa cells in TP Mode. λ_{em} = 570–620 nm; λ_{ex} = 561 nm in OP mode and 730 nm in TP mode. Scale bar: 25 μm.

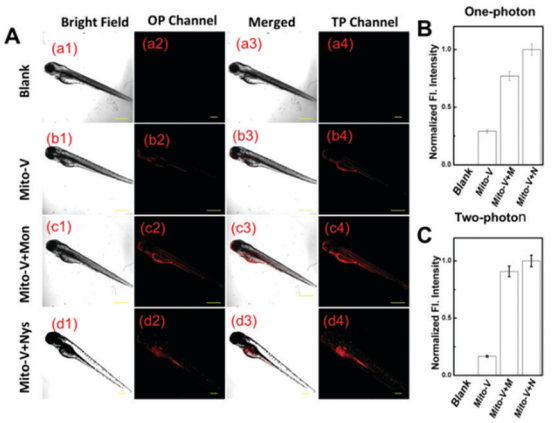

Fig. 5 (a1)–(a4) Confocal fluorescence images of the zebrafish incubated without **Mito-V**. (b1)–(b4) Confocal fluorescence images of the zebrafish incubated with 10 μM **Mito-V**. (c1)–(c4) Confocal fluorescence images of the zebrafish incubated with 10 μM monensin for 30 min + 10 μM **Mito-V** for another 30 min. (d1)–(d4) Confocal fluorescence images of the zebrafish incubated with 10 μM nystatin for 30 min + 10 μM **Mito-V** for another 30 min. OP: λ_{ex} = 561 nm; TP: λ_{ex} = 730 nm; scale bar =250 μm.

Published on 04 October 2019. Downloaded by University of Georgia on 1/3/2020 6:36:17 AM.

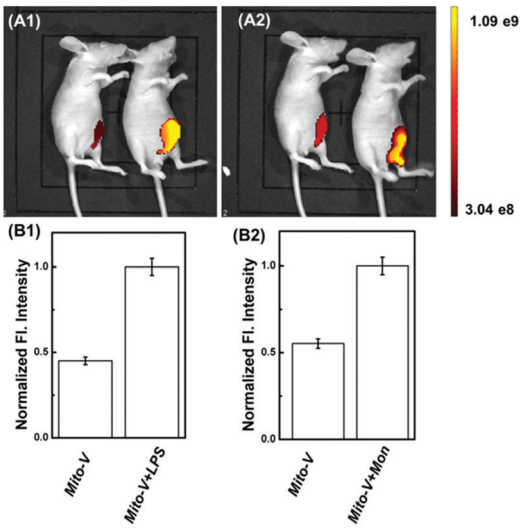

Fig. 6 (A1) Normal living mice + probe **Mito-V** (left) and mice triggered with LPS + probe **Mito-V** (right); (A2) normal living mice + probe **Mito-V** (left) and mice triggered with monensin + probe **Mito-V** (right); B1 refers to the normalized fluorescence intensity of mice in A1 and B2 refers to the normalized fluorescence intensity of mice in A2. Error bars represent standard deviation (±S.D.), n = 3, the statistical analysis was performed on three separate biological replicates. λ_{ex} = 520 nm, λ_{em} = 670 nm.

Encouraged by the above results, tracking viscosity in mice was also performed. As reported in the previous literature, inflammation can stimulate an increase in the viscosity of a biological system with the trigger of Lipopolysaccharide (LPS).[34] To further study the feasibility of **Mito-V** to monitor the viscosity changes *in vivo*, LPS was injected into nude mice to induce inflammation The normal mice and inflamed mice stimulated with LPS or monensin emitted inconspicuous fluorescence (Fig. S7(a1 and a2), ESI†). However, after injection of **Mito-V**, the inflamed mice incubated with LPS exhibited obvious stronger fluorescence than the normal mice (Fig. 6(A1)). In addition, monensin was also utilized to induce increased viscosity in the nude mice, and the results corresponded well with LPS observations (Fig. 6A2). Furthermore, the analysis results of the inflamed mice demonstrated that the fluorescence intensity was about 2.1-fold higher than for the normal mice (Fig. 6(B1 and B2)). These results collectively demonstrate that **Mito-V** could be applied for monitoring viscosity *in vivo*.

In summary, a two-photon and mitochondria-targeting fluorescent probe, **Mito-V,** was designed for sensing the viscosity changes in cells and *in vivo*. The probe exhibited a 22-fold enhancement with the increase of viscosity from 1.4 cP to 956 cP. More interestingly, with the powerful sensor **Mito-V**, the detection of mitochondrial viscosity has been successfully achieved not only in living cells but also *in vivo*. Thus, **Mito-V** is a promising tool for sensing viscosity in complex biological systems.

Conflicts of interest

There are no conflicts to declare.

Acknowledgements

This work was financially supported by NSFC (21472067, 21672083, 21877048), Taishan Scholar Foundation (TS201511041), and the startup fund of University of Jinan (309-10004). The animals were purchased from School of Pharmaceutical Sciences, Shandong University, and the studies were approved by the Animal Ethical Experimentation Committee of Shandong University. All animals were kindly kept during experiment according to the requirements of the National Act on the use of experimental animals (China).

Notes and references

1 T. Aron, K. M. Ramos-Tottes, J. A. Cotruvo Jr. and C. J. Chang, *Acc. Chem. Res.*, 2015, **48**, 2434–2442.
2 P. Ning, J. C. Jiang, L. C. Li, S. X. Wang, H. Z. Yu, Y. Feng, M. Z. Zhu, B. C. Zhang, H. Yin, Q. X. Guo and X. M. Meng, *Biosens. Bioelectron.*, 2016, **77**, 921–927.
3 Z. G. Yang, Y. X. He, J. H. Lee, N. Y. Park, M. Suh, W. S. Chae, J. F. Cao, X. J. Peng, H. Jung, C. Kang and J. S. Kim, *J. Am. Chem. Soc.*, 2013, **135**, 9181–9185.
4 P. Ning, P. Y. Dong, Q. Geng, L. Bai, Y. Q. Ding, X. H. Tian, R. Shao, L. Li and X. M. Meng, *J. Mater. Chem. B*, 2017, **5**, 2743.
5 A. Jiménez-Sánchez, E. K. Lei and S. O. Kelley, *Angew. Chem., Int. Ed.*, 2018, **57**, 8891–8895.
6 N. Gupta, S. I. Reja, V. Bhalla, M. Gupta, G. Kaur and M. Kumar, *J. Mater. Chem. B*, 2016, **11**, 1968–1977.
7 J. P. Li, Y. Y. Zhang, H. Zhang, X. P. Xuan, M. S. Xie, S. Xia, G. R. Qu and H. M. Guo, *Anal. Chem.*, 2016, **88**, 5554–5560.
8 S. J. Chen, Y. N. Hong, Y. Zeng, Q. Q. Sun, Y. Liu, E. G. Zhao, G. X. Bai, J. N. Hao and Z. Tang, *Chem. – Eur. J.*, 2015, **21**, 4315–4320.
9 O. Morawski, B. Kozankiewicz, A. Miniewica and A. L. Sololewski, *Chem. Phys. Chem.*, 2015, **16**, 3500–3510.
10 Roopa, N. Kumar, V. Bhalla and M. Kumar, *Chem. Commun.*, 2015, **51**, 15614–15628.
11 L. H. Feng, Y. Wang, F. Liang, X. J. Wang and L. W. Zhang, *Sens. Actuators, B*, 2011, **156**, 499–503.
12 H. L. Liu, Q. Peng, Y. D. Wu, D. Chen, X. L. Hou, M. Sabat and L. Pu, *Angew. Chem., Int. Ed.*, 2010, **49**, 602–606.
13 Y. Ooyama, S. Inoue, T. Nagano, K. Kushimoto, J. Ohshita, I. Imae, K. Komaguchi and Y. Harima, *Angew. Chem., Int. Ed.*, 2011, **50**, 7429–7433.
14 X. B. Song, N. Li, C. Wang and Y. Xiao, *J. Mater. Chem. B*, 2017, **5**, 360–368.
15 S. C. Lee, J. Y. Heo, J. W. Ryu, C. L. Lee, S. Kim, J. S. Tae, B. O. Rhee, S. W. Kim and O. P. Kwon, *Chem. Commun.*, 2016, **52**, 13695–13698.
16 D. D. Li, X. H. Tian, A. D. Wang, L. J. Guan, J. Zheng, F. Li, S. L. Li, H. P. Zhou, J. Y. Wu and Y. P. Tian, *Chem. Sci.*, 2016, **7**, 2257–2263.
17 L. Yuan and W. Lin, *Biomaterials*, 2013, **34**, 9566–9571.
18 H. Chen, Y. Tang and W. Lin, *TrAC, Trends Anal. Chem.*, 2016, **16**, 1397–1406.
19 M. Xue and K. L. Wang, *Senors*, 2012, **12**, 11612–11637.

 This journal is © The Royal Society of Chemistry and the Centre National de la Recherche Scientifique 2019

Published on 04 October 2019. Downloaded by University of Georgia on 1/3/2020 6:36:17 AM.

20 M. K. Kuimova, S. W. Botchway, A. W. Parker, M. Balza, H. A. Collins, H. L. Anderson, K. Suhling and P. R. Ogilby, *Nat. Chem.*, 2009, **1**, 69–73.
21 M. Ren, B. Deng, K. Zhou, X. Kong, J. Wang, G. Xu and W. Lin, *J. Mater. Chem.*, 2016, **4**, 4739–4745.
22 M. Ren, B. Deng, K. Zhou, X. Kong, J. Wang and W. Lin, *Anal. Chem.*, 2017, **89**, 552–555.
23 X. J. Peng, Z. G. Yang, J. Y. Wang, J. L. Fan, Y. X. He, F. L. Song, B. S. Wang, S. G. Sun, J. L. Qu, J. Qi and M. Yan, *J. Am. Chem. Soc.*, 2011, **133**, 6626–6635.
24 M. A. Haidekker, T. P. Brady, D. Lichlyter and E. A. Theodorakis, *J. Am. Chem. Soc.*, 2005, **128**, 398–399.
25 G. S. Kottas, L. I. Clarke, D. Horinek and J. Michl, *Chem. Rev.*, 2005, **105**, 1281–1376.
26 Y. Baek, S. J. Park, X. Zhou, G. Kim, H. M. Kim and J. Yoon, *Biosens. Bioelectron.*, 2016, **86**, 885–891.
27 M. G. Ren, K. Zhou, L. Wang, K. Y. Liu and W. Y. Lin, *Sens. Actuators, B*, 2018, **262**, 452–459.
28 N. Jiang, J. L. Fan, S. Zhang, T. Wu, J. Y. Wang, P. Gao, J. L. Qu, F. Zhou and X. J. Peng, *Sens. Actuators, B*, 2014, **190**, 685–693.
29 W. Sun, Y. D. Shi, A. X. Ding, Z. L. Tan, H. Chen, R. Liu, R. B. Wang and Z. L. Lu, *Sens. Actuators, B*, 2018, **276**, 238–246.
30 F. Liu, Y. S. Luo and M. Y. Xu, *Tetrahedron Lett.*, 2018, **59**, 4540–4544.
31 L. Wang, Y. Xiao, W. M. Tian and L. Z. Deng, *J. Am. Chem. Soc.*, 2013, **135**, 2903–2906.
32 S. P. Soltoff and L. J. Mandel, *J. Membr. Biol.*, 1986, **94**, 153–161.
33 J. G. Molina, X. L. Zhang, M. Borghesan, J. M. D. Silva, M. Awan, B. Fuller, N. Gavara and C. Selden, *Biomaterials*, 2018, **177**, 113–124.
34 E. Yeom, H. M. Kim, J. H. Park, W. Choi, J. Doh and S. J. Lee, *Sci. Rep.*, 2017, **7**, 1801.